Three-Dimensional Quantitative Structure−Activity Relationship Analysis of Ligand Binding to Human Sequence Antidigoxin Monoclonal Antibodies Using Comparative Molecular Field Analysis

Carol D. Farr, Michael R. Tabet, and William J. Ball, Jr.*

Department of Pharmacology and Cell Biophysics, University of Cincinnati College of Medicine, Cincinnati, Ohio 45267-0575

Dianne M. Fishwild[†]

GenPharm International/Medarex, San Jose, California 95131

Xia Wang,[‡] Anil C. Nair,[§] and William J. Welsh[‖]

Department of Chemistry and Center for Molecular Electronics, University of Missouri-St. Louis, St. Louis, Missouri 63121

The present study indicates that the newly generated human sequence antidigoxin monoclonal antibody (mAb), 1B3, binds digoxin with a different fine specificity binding than our previously obtained human sequence monoclonal antibodies (mAbs) (Ball, W. J.; et al. *J. Immunol.* **1999**, *163*, 2291−2298). Uniquely, 1B3 has a higher affinity for digitoxin than digoxin, the immunizing hapten, and a strong requirement for at least one sugar residue linked to the aglycone (-genin). By means of comparative molecular field analysis (CoMFA), the results of competition binding studies for 56 cardiotonic and hormonal steroids were employed to develop three-dimensional quantitative structure−activity relationship (3D-QSAR) models for ligand binding to 1B3 and to three additional human sequence mAbs, as well as the murine antidigoxin mAb 40-50 (Mudgett-Hunter, M.; et al. *Mol. Immunol.* **1985**, *22*, 447−488). All five 3D-QSAR models yielded cross-validated q^2 values greater than 0.5, which indicates that they have significant predictive ability. The CoMFA StDev*Coeff contour plots, as well as the competition results, indicate that 1B3 binds ligands in a manner distinct from the other four mAbs. The CoMFA contour plots for 40-50 were also compared with the known X-ray crystallographic structure of the 40-50−ouabain complex (Jeffrey, P. D.; et al. *J. Mol. Biol.* **1995**, *248*, 344−360) in order to identify correlations between residues in the mAb binding site and specific contour plot regions. These 3D-QSAR models and their respective contour plots should be useful tools to further understand the molecular nature of antibody−antigen interactions and to aid in the redesign or enhancement of therapeutic antibodies.

Introduction

Congestive heart failure (CHF) is a progressive, highly lethal condition that currently affects over nine million Americans, Europeans, and Japanese. Furthermore, the incidence of CHF is expected to continue to increase as the populations of these countries age.[1,2] Even with recently developed treatments that include angiotensin-converting enzyme (ACE) inhibitors and angiotensin II receptor antagonists, CHF continues to have a 5 year mortality rate of 50%.[1] The original inotropic preparation used in CHF, digitalis, which acts through inhibition of Na^{+},K^{+}-ATPase, contains the active compounds digoxin and digitoxin. Worldwide, both compounds are among the most frequently pre-scribed drugs and they continue to play a primary role in CHF treatment.[3−5] Unfortunately, digoxin and digi-toxin have a narrow therapeutic index,[6] and currently, patients with life-threatening digitalis overdoses are treated with sheep polyclonal antidigoxin antibody fragments (Fabs).[7] These Fabs, infused intravenously, bind and inactivate free drug and shift the equilibrium between free drug and receptor-bound drug. The result is a reduction in the level of receptor-bound drug and an acceleration in the rate of drug excretion. In addition, polyclonal and monoclonal antidigoxin antibodies (mAbs) are used in immunoassays to monitor serum digoxin levels in patients.[8] This information is critical for the proper maintenance of therapeutically safe concentra-tions. Unfortunately, the clinical use of sheep polyclonal antidigoxin Fabs is limited because of concerns about the safety of repeated use of foreign species proteins in patients and possible variations in a polyclonal prod-uct.[9−11]

Fabs derived from human sequence antidigoxin mAbs, with less potential for hypersensitive reactions (acute anaphylaxis or delayed serum sickness)[10] and the de-sired affinity, specificity, and elimination rate,[11] should

---

* To whom correspondence should be addressed. Tel.: (513)558-2388. Fax: (513)558-1169. E-mail: William.Ball@uc.edu.
† Current address: Affymax Research Institute, Santa Clara, Cali-fornia 95051.
‡ Current address: AstraZeneca Pharmaceuticals, 1800 Concord Pike, Wilmington, DE 19850.
§ Current address: Aventis Pharmaceuticals, 1580 E. Hanley Blvd., Tuscon, AZ 85737.
‖ Current address: Department of Pharmacology, Medicine, and Dentistry, Robert Wood Johnson Medical School, University of Medi-cine & Dentistry, 675 Hoes Lane Piscataway, NJ 08854.

Table 1. Dissociation Constant (K_D) Values and Inhibition Constant (K_I) Values for mAb 1B3 as Determined by Radioligand ([^{3}H]Digoxin and [^{3}H]Digitoxin) Binding Assays

	K_D (nM)		K_I (nM)				
Mab	digoxin	digitoxin	digoxin	digitoxin	digoxigenin	digitoxigenin	progesterone
1B3	3.1 ± 0.1	0.6 ± 0.1	1.2 ± 0^a	0.1 ± 0.03^a	3100 ± 140^a	1000 ± 80^a	$36\,000 \pm 22\,000^a$
			0.8 ± 0.1^b	0.2 ± 0^b	1700 ± 30^b	880 ± 220^b	nd^c

^{a} Determined against [^{3}H]digoxin. ^{b} Determined against [^{3}H]digitoxin. ^{c} nd for not determined.

be a safer and more effective treatment for digitalis overdose. Therefore, we have recently generated a collection of human sequence antidigoxin IgG mAbs, using transgenic mice with humanized humoral systems, as possible improvements over the sheep-derived Fab products. We have previously reported an initial characterization of six human mAbs, including their fine-binding specificities and K_D values for digoxin.[12] In this paper, we report the characterization of an additional human mAb, designated 1B3, that has a higher affinity (subnanomolar K_D) for digitoxin than for digoxin (the hapten on the immunogen). This preference for digitoxin distinguishes 1B3 from the other six human sequence mAbs.

Because a key element in the clinical and diagnostic usefulness of mAbs and Fabs is their binding affinity and specificity,[11] there is considerable interest in understanding the structural basis of antibody–drug complex formation.[13] Margolies and colleagues have used a collection of murine antidigoxin mAbs and engineered mAbs to compare the primary structure of the binding site for the ligand with the specificity for digoxin. In addition, the availability of a large number of natural and synthetic cardiotonic steroids has made it possible to determine the fine binding specificities of several of these mAbs.[14–17] Three-dimensional (3D) structural determinations using X-ray crystallography have provided further insight into how two of the murine Fabs, 40-50 and 26-10, bind ouabain and digoxin, respectively.[17,18]

Here, we report the first use of comparative molecular field analysis (CoMFA) to develop 3D quantitative structure–activity relationship (QSAR) models that correlate structure-based parameters of cardiotonic and hormonal steroids with their affinities for mAb 1B3 and several additional antidigoxin mAbs. Two major structure-based parameters, the steric and electrostatic fields surrounding each compound, were calculated using CoMFA.[19] The activity values of the ligands were based on their ability to inhibit digoxin binding to the mAbs, as determined by enzyme-linked immunosorbent assay (ELISA) competition binding experiments. The CoMFA also generates StDev*Coeff contour plots that visualize the regions where variations in the structure-based fields are most highly correlated with the variations in the ligands' biological activities.[19–21] CoMFA is a compelling tool for examining receptor–ligand interactions, for new drug design and for other QSAR applications.[21–28] We suggest that an examination of the contour plots can also provide information about the antibody's structural contribution to affinity and specificity and provide a basis for the redesigning of therapeutic antibodies.

In addition to the CoMFA-based 3D-QSAR model for 1B3, we developed models for three (of the original six) additional human sequence antidigoxin mAbs, 7F2,

11E6, and 5C2,[12] and one murine mAb, 40-50.[17] Digoxin is composed of a cardenolide type four ring steroid moiety with the A–B and C–D rings joined in a cis, nonhormonal configuration, while the B and C rings are joined in the trans configuration.[29] Digoxin has three $\beta(1,4)$-D-glycoside-linked digitoxoses attached at the C-3 oxygen and an α,β-unsaturated five member lactone ring attached at C-17 (Figure 1A). The cardiotonic steroids used as competitors have substitutions at various positions on the steroid rings, different numbers and types of carbohydrates at C-3, and variations in the saturation and size of the lactone ring (Figure 1A; Table 2A). The characteristic structure of hormonal steroid rings A–D is a flattened, all trans arrangement, although the A ring of progesterone analogues has been shown to project at various angles from the other three rings.[15,30] Each antibody's binding site for these compounds is formed by their complementarity determining regions (CDRs) of the heavy and light chain variable domains. The noncovalent complex formation is achieved with electrostatic interactions, structural complementarity,[31] and, sometimes, small orientation or conformational changes within the CDRs[32] and the ligands. However, we note that with the murine 40-50 Fab both digoxin and ouabain appear to occupy a similar position in the Fab–ligand complex, without major structural rearrangements of the ligand or Fab.[17]

The CoMFA contour plots generated by our binding data clearly illustrate the similarities and differences in the manner in which the human sequence mAbs and the murine mAb bind digoxin. The similarities suggest that there may be structural requirements for a high-affinity digoxin binding site that limit the extent of sequence variations possible between mAbs. This is consistent with the observation that there are preferred amino acid residues in the CDR regions, especially aromatic groups, and a limited number of main chain conformations.[33] In addition to the overall similarities of the contour plots, there are distinctive regions that clearly distinguish 1B3 from the other three human mAbs and also distinguish between the similar mAbs 7F2 and 11E6. These differences in the CoMFA contour plots may be correlated with limited site specific differences in the primary sequences of the human sequence antidigoxin mAbs. Therefore, the 3D-QSAR contour plots may suggest strategies for selecting specific site-directed mutations of the mAbs that could enhance their binding affinities or alter their specificities in order to generate a clinical antidote with broadened usefulness. Understanding the structural features that contribute to antibody–ligand recognition will assist this development.

Materials and Methods

Transgenic Mice. The development of the transgenic mouse strain designated HC2/KCo5, with inactivated endogenous mouse μ heavy and κ light chain loci and inserted human
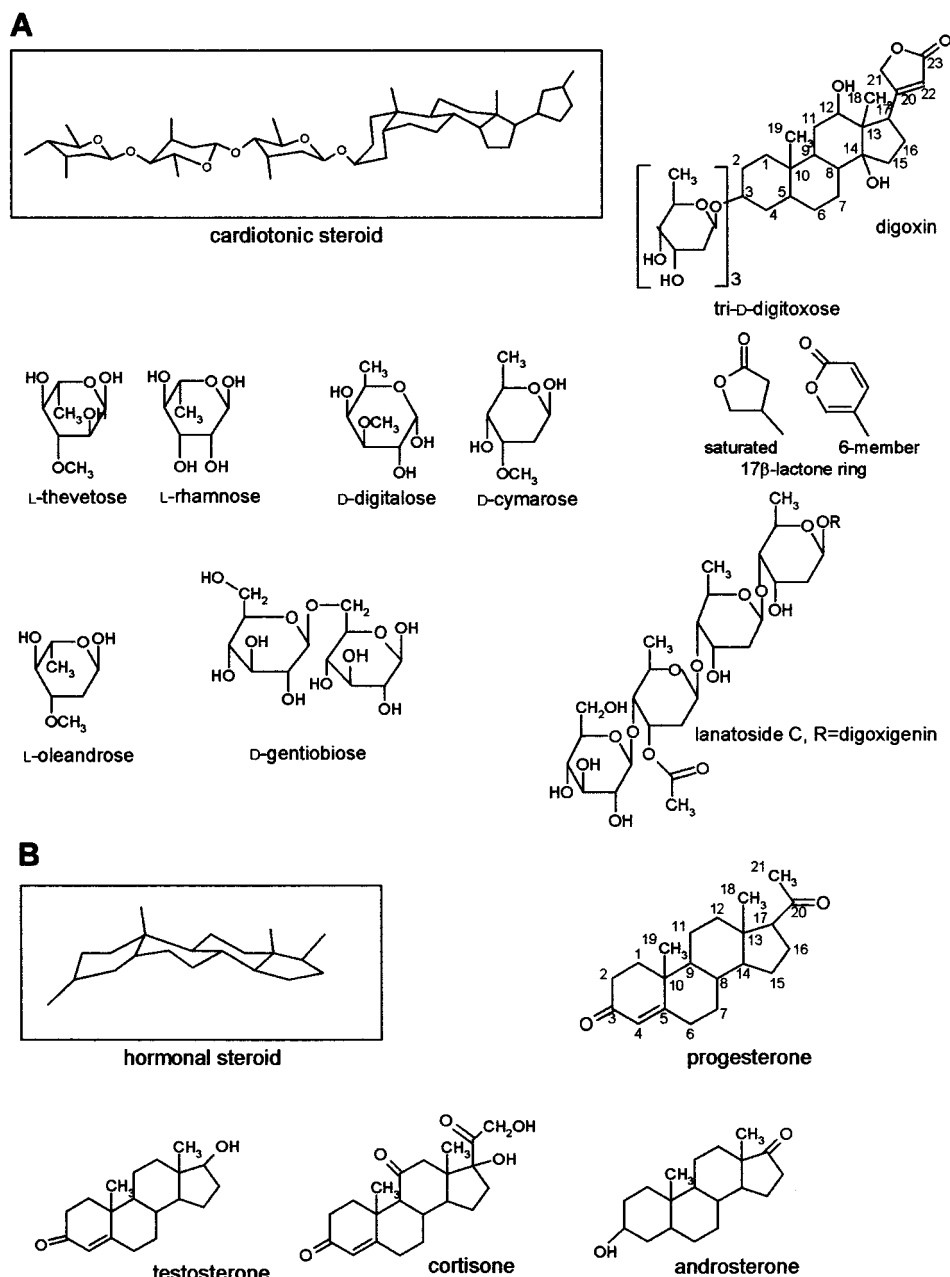
Figure 1. Structures of the cardiotonic steroid and hormonal steroids. (A) The structure of digoxin (boxed), illustrating the cis−trans−cis conformation and selected sugar and lactone ring substitutions from Table 2A. (B) The structure of progesterone (boxed), illustrating the all trans conformation and representative hormonal steroids from Table 2B.

μ and $\gamma 1$ heavy and κ light chain transgenes, has been previously described.[34−36]

Immunization, Cell Fusion, Cloning, and Characterization of Human mAbs. The HC2/KCo5 mice were immunized with digoxin conjugated to keyhole limpet hemocyanin (digoxin−KLH). The hybridoma cell line designated as 1B3-18 was produced and cloned as previously described.[12,36] The secreted human sequence mAb, 1B3, was then characterized using ELISAs to establish its specificity for the hapten digoxin and its isotype as a human IgG₁ (κ) immunoglobulin.[12,36] The human sequence mAbs 7F2, 11E6, and 5C2 were purified using protein A-Sepharose column chromatography, while 1B3, due to limited quantities, was used directly from cell culture spent media.

Avidity Determinations. The avidity of 1B3 for digoxin was determined using an ELISA in which digoxin, conjugated to bovine serum albumin (digoxin−BSA), was adsorbed to microtiter plates. Complex formation between the mAb and

the hapten was detected with biotinylated goat antihuman IgG₁ specific antibodies (Abs) and quantitated as previously described.[12]

Competitive Binding ELISAs. The inhibition constants of the human sequence antidigoxin mAbs for various cardiotonic steroids and hormonal steroids were determined with a competitive binding ELISA. Goat antihuman IgG Fc-region specific IgG (3.5 μg/mL; 100 μL/well) in 1 mM ethyleneglycol-bis-(β-aminoethyl)-N,N,N,N-tetraacetic acid (EGTA; pH 7.4) was adsorbed onto (poly)vinyl chloride microtiter plates for 1 h. Then, the plates were blocked for 10 min with 0.5% BSA in Tris-buffered saline [TBS; 10 mM Tris(hydroxymethyl aminomethane) base, 140 mM NaCl, 0.02% NaN₃, pH 7.4]. To capture the human sequence mAbs to the plate, 100 μL of TBS-diluted (including 0.5% BSA) mAb (∼0.5 μg/mL) was added to each well and the plate was incubated for 1 h. Next, digoxin−alkaline phosphatase conjugate (1/40 dilution; 100 μL/well; O. E. M. Concepts, Toms River, NJ) and varying concentrations

Table 2. Structural Characteristics of Cardiotonic Steroids and Hormonal Steroids

Section A: Cardiotonic Steroids

cardiotonic steroid	1β	3β	5β	11α	12β	16β	17β	19
digoxigenin base								
digoxin		tri-D-digitoxose			−OH			
α-acetyldigoxin		tri-D-digitoxose[a]			−OH			
lanatoside C		see Figure 1B			−OH			
12-acetyldigoxin[b]		tri-D-digitoxose			−OCOCH3			
dihydrodigoxin[b]		tri-D-digitoxose			−OH		saturated	
digoxigenin bis- digitoxose		bis-D-digitoxose			−OH			
digoxigenin mono-digitoxose		D-digitoxose			−OH			
digoxigenin		−OH			−OH			
dihydrodigoxigenin[b]		−OH			−OH		saturated	
3-epidigoxigenin[b]		α-OH[c]			−OH			
digoxigenin-3,12-diacetate		−OCOCH3			−OCOCH3			
digitoxigenin base								
digitoxin		tri-D-digitoxose						
acetyldigitoxin (α:β − 2:1)		tri-D-digitoxose[a]						
dihydrodigitoxin		tri-D-digitoxose					saturated	
digitoxigenin bis-digitoxose		bis-D-digitoxose						
digitoxigenin mono-digitoxose		D-digitoxose						
evomonoside		L-rhamnose						
neriifolin		L-thevetose						
thevetin B		one thevetose + one (2 sugar) gentiobiose						
digitoxigenin		−OH						
acovenoside A[b]	−OH	6-deoxy-3-O-methyl-L-talose						
uzarigenin (*trans* A/B ring)		−OH	α-H					
bufalin		−OH					six member[d]	
cinobufagin		−OH	−OH			−OCOCH3	six member[d] 14−15 β-epoxide	
proscillaridin A		L-rhamnose	4−5 double bond				six member[d]	
gitoxigenin base								
gitoxin		tri-D-digitoxose				−OH		
diginatin[b]		tri-D-digitoxose			−OH	−OH		
gitaloxin[b]		tri-D-digitoxose				−OCHO		
16-acetylgitoxin		tri-D-digitoxose				−OCOCH3		
gitoxigenin-3-acetate[b]		−OCOCH3				−OH		
gitoxigenin		−OH				−OH		
strospeside[b]		D-digitalose				−OH		
oleandrigenin mono-digitoxose[b]		D-digitoxose				−OCOCH3		
oleandrin		oleandrose[e]				−OCOCH3		
oleandrigenin[b]		−OH				−OCOCH3		
strophanthidol[b]		−OH	−OH					−OH
strophanthidin		−OH	−OH					=O
acetylstrophanthidin		−OCOCH3	−OH					=O
helveticoside		D-digitoxose	−OH					=O
ouabain	−OH	L-rhamnose	−OH	−OH				−OH
ouabagenin	−OH	−OH	−OH	−OH				−OH

Section B: Hormonal Steroids

hormonal steroid	3	4 to 5, 5 to 6, or 6 to 7 double bond	6	11β	17	18
androsterone	α-OH	none			=O	
dehydroisoandrosterone[f]	β-OH	5−6			=O	
progesterone	=O	4−5			β-COCH3	
chlormadinone acetate	=O	4−5; 6−7	−Cl		α-OCOCH3; β-COCH3	
17α-hydroxyprogesterone 17-acetate 3-(O-carboxymethyl)oxime	NOCH2CO2H	4−5			α-OCOCH3; β-COCH3	
testosterone	=O	4−5			β-OH	
corticosterone	=O	4−5		−OH	β-COCH2OH	
aldosterone[g]	=O	4−5		−OH	β-COCH2OH	=O
dehydrocortisone[h]	=O	1−2; 4−5		=O	α-OH; β-COCH2OH	
prednisolone 21-acetate	=O	1−2; 4−5		−OH	α-OH; β-COCH2OCOCH3	
prednisolone 21-hemisuccinate	=O	1−2; 4−5		−OH	α-OH; β-COCH2OCO(CH2)2COO−	
hydrocortisone	=O	4−5		−OH	α-OH; β-COCH2OH	
cortisone	=O	4−5		=O	α-OH; β-COCH2OH	
cholesterol	β-OH	5−6			β-CH(CH3)(CH2)3CH(CH3)2	
β-estradiol[i]	−OH	aromatic A ring			β-OH	

[a] α or β -OCOCH3 on terminal digitoxose C-3. [b] Analogues used only in Margolies' lab data set.[17] [c] Note α orientation. [d] See Figure 1B. [e] (2,6-Dideoxy-3-O-methyl-α-L-arabino-hexopyranosyl)oxy. [f] Prasterone. [g] In equilibrium with hemiacetal formed by C-11 hydroxyl and C-18 carboxyl (we used structure of hemiacetal). [h] Prednisone. [i] Note: no methyl on C-10.

of digoxin or competitor in TBS (including 0.5% BSA) were added and incubated for 2 h. Each competitor was initially dissolved in chloroform, ethanol, methanol, or water according to its individual solubility and then diluted in TBS. Finally, the plates were washed to remove unbound conjugate and 50 μL of *p*-nitrophenyl phosphate (PNPP) substrate (1 mg/mL PNPP, 50 mM Na_2CO_3, 50 mM $NaHCO_3$, and 1 mM $MgCl_2$ at pH 9.8) was added to each well. The colorimetric reaction time was determined by observing the color development and varied (8−25 min), depending on the mAb used. The reaction was stopped with 1 N NaOH (50 μL/well). All steps were performed at room temperature. The reaction endpoint was measured with a Molecular Devices ELISA Reader at a wavelength of 405 nm. Optical density (OD) values were determined in duplicate at various inhibitor concentrations and normalized using "1" as the maximum value obtained with no inhibitor present. The data were analyzed with a four parameter logistic equation using Kaleidagraph (Synergy Software, Reading, PA).

The IC_{50} ratios reported are the ratio of the IC_{50} for the inhibitor to that for digoxin as determined on the same assay plate. Thus, for each mAb, the IC_{50} ratio for digoxin is "1" and inhibitors with lower affinities have IC_{50} ratios greater than "1". Each reported ratio is the average ratio determined in 3−5 separate experiments. The fractional standard error of the mean (SEM) for each competitor was ±0.3 of the ratio value. The data reported here include IC_{50} ratio values initially reported for 7F2, 11E6, and 5C2[12] plus additional repetitions and an expanded group of inhibitors.

In addition, because the X-ray crystallographic structure of 40-50 complexed with ouabain is available, a 3D-QSAR model was developed for 40-50, using the radioligand competition assay data that was generated previously by Jeffrey and colleagues.[17] These data were reported as relative K_i values using the ratios of the K_i values for the inhibitors vs the K_i for digoxin.

Radioligand Binding Assays. The dissociation constants (K_D values) of 1B3 for digoxin and digitoxin were determined with a radioligand binding assay that uses a double antibody precipitation technique. To confirm the K_D results, the inhibition constant (K_I) for several compounds was determined using a radioligand competition binding assay. Both assays were performed as previously described[12] with minor modifications. The reaction mixture volumes were 2.0 mL, and the concentration of 1B3 was less than 0.1 K_D. The K_D values were determined by fitting the equilibrium binding assay data points with a rectangular hyperbolic curve using KaleidaGraph (Synergy Software). For the competition binding assay, the molar concentration of inhibitor needed to reduce mAb−radioligand binding by 50% (IC_{50}) was determined by fitting the data points with a four parameter logistic equation using Kaleidagraph (Synergy Software). Then, the K_I values were calculated with the Cheng and Prusoff equation.[37] The reported K_D and K_I values are the averages of at least two independent experiments. The errors are the average deviations of the mean.

Training Sets for QSAR Analysis. The training sets (i.e., the competition binding data sets) used to construct the 3D-QSAR models for the four human sequence mAbs are developed from the determined IC_{50} ratios. The training set for the 40-50 is from the relative K_i values reported by Jeffrey and colleagues.[17] To be consistent with other 3D-QSAR studies, the IC_{50} ratios and relative K_i values were converted so that high activity values matched high affinity values. The training set data point for each competitor was calculated as log [100 × (IC_{50} of digoxin/IC_{50} of inhibitor)], which equals log(100/ IC_{50} ratio) or log(100/rel. K_i). For example, the training set data value point for digoxin is 2, the log 100, and competitors with lower affinity have lower values.

Two 3D-QSAR models were constructed for each human sequence and murine mAb. The first model (model I) was developed by dividing the data set into a training set I (22−33 compounds) for model construction and a test set I of four and three compounds, respectively, for the human and mouse

mAbs, for model validation. The second model (model II) was constructed from the entire data set (training set II).

Molecular Modeling. The 3D structure of each compound was built using the molecular fragment library of Sybyl 6.6 (Tripos, Inc., St. Louis, MO) on a Silicon Graphics workstation. The structure of each cardiotonic steroid was based on the X-ray crystallographic structure of digoxin as bound to murine Fab 26-10,[18] available (identification number 1IGJ) in the Protein Data Bank (PDB). The orientation of the lactone ring was initially set similar to that for the 40-50−ouabain complex.[17] The structure of each hormonal steroid was based on the X-ray crystallographic structure of progesterone as bound to Fab DB3,[38] available (identification number 1DBB) in the PDB. Because Jeffrey and colleagues did not observe any electron density for the two terminal digitoxoses in the structure of digoxin, two digitoxose sugars were added to the PDB structure, using the molecular fragments library in Sybyl. Then, the global minimum energy conformation was determined using the following steps: (i) optimized geometry of digoxin to the local minimum energy conformation to an energy gradient of 0.001 kcal/mol Å, (ii) searched all rotatable bonds in 10° increments to locate minimum energy torsion angles, and (iii) reoptimized the structure to its lowest minimum energy conformation, using the bond angles established in step two. The energy-minimized structure of digoxin was modified with the molecular fragments library to build the remaining cardiotonic steroid structures. A global minimum energy conformation was also determined for thevetin B because of the 1-6 glycosidic bonds created a twisted carbohydrate chain. Similarly, the progesterone structure was modified to build the additional steroid structures. Finally, all structures were energy-minimized using the Tripos force field with a distance-dependent dielectric function and a convergence criterion of 0.001 kcal/mol energy difference between successive iterations. The Gasteiger−Marsili method was used to calculate the atomic partial charges.[39] Although there can be rotation about the glycoside (C-3, O) and lactone−cardenolide (C-17 to C-20) bonds, we assumed the same conformation for each bound compound with each mAb. We compared the contour plot for each mAb, with the understanding that a C-3 or C-17 rotation may have occurred.[29]

CoMFA Alignment. The alignment procedure matched the B and C rings (C-5 to C-14) of each cardiotonic and hormonal steroid to the corresponding atoms in digoxin, using a least squares fit. Therefore, these rings served as the scaffolding of the pharmacophoric elements. A composite diagram of all of the aligned compounds is shown in Figure 3. Next, each compound was independently placed in a 3D grid with 2 Å spacing intervals. A carbon probe with a sp^3 configuration and a +1.0 charge was placed at each grid intersection and the steric (van der Waals 6-12) and electrostatic (Coulombic terms, with a distance-dependent (1/r) dielectric function) energies between the probe and the compound were calculated for each intersection. The calculated energies greater than 30 kcal/mol were truncated to this value. These calculations established the steric and electrostatic fields surrounding each compound.

Partial Least Squares (PLS) QSAR. PLS regression was used to analyze the CoMFA results by correlating variations in the determined relative affinity values with variations in the steric and electrostatic fields of the corresponding compound. The analysis generates a linear equation,[20]

$$\text{biological activity} = k + aS_1 + bS_2 + ... + mS_n + nE_1 + ... + zE_n \quad (1)$$

where k is a constant, $a-m$ are the coefficients for the steric (S) parameters, and $n-z$ are the coefficients for the electrostatic (E) parameters. A PLS cross-validation procedure (leave-one-out, LOO) combined and reduced the large number of steric and electrostatic field descriptors to a few principal components (PCs), linear combinations of the original descriptor variables that can be used to establish a linear relationship with the log values. The q^2 value (eq 2) shows how well the model-predicted values match the observed values:
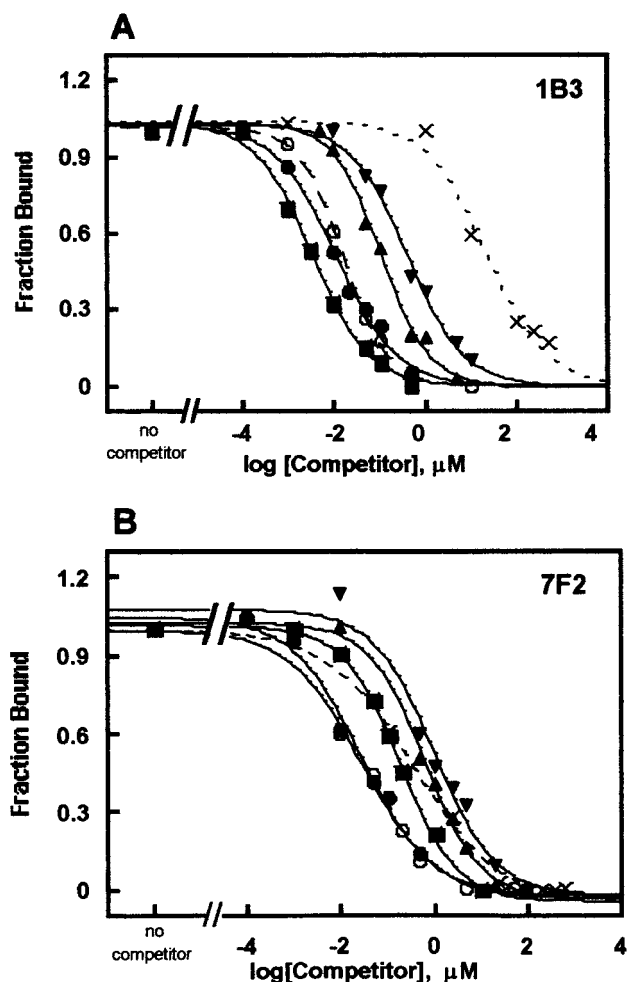
Figure 2. Representative examples of competition ELISA determinations of the binding specificities of mAbs 1B3 (A) and 7F2 (B). The curves show the ability of digoxin and various digitoxin-related compounds to inhibit digoxin–alkaline phosphatase conjugate binding to each mAb. The fraction of bound dig–AP was plotted for each increasing concentration of digoxin (O, ●), digitoxin (■), digitoxigenin bis-digitoxoside (▲), digitoxigenin monodigitoxoside (▼), and digitoxigenin (×). Each point is the average of two determinations. The curves were generated by the fit of a four parameter logistic equation to the data points for each competitor.

$$q^2 = 1 - [\sum (y - y_{pred})^2 / \sum (y - y_{mean})^2] \qquad (2)$$

where y, y_{pred}, and y_{mean} represent each observed value, each predicted value, and the mean descriptor value, respectively.[20] Models with significant ability to predict the activity of untested compounds generally have a $q^2 > 0.5$.[21] The final predictive 3D-QSAR model was determined with the LOO-determined number of PCs and without cross-validation. The r^2 value (eq 3) shows the goodness of fit (i.e., the validity of the correlation between the calculated steric and electrostatic fields and the log value):

$$r^2 = 1 - [\sum (y - y_{cal})^2 / \sum (y - y_{mean})^2] \qquad (3)$$

where y, y_{cal}, and y_{mean} represent each observed log value, each predicted log value based on the final 3D-QSAR equation, and the descriptor mean value, respectively. A $r^2 > 0.9$ is considered to be internally self-consistent.[21]

The initial 3D-QSAR models developed for the five mAbs included the entire set of IC$_{50}$ ratio data, but three of the models did not meet the generally accepted criteria ($q^2 > 0.5$, $r^2 > 0.9$).[21] Therefore, two (digitoxin and digoxigenin-3,12-

diacetate), one (digoxigenin-3,12- diacetate), and three (digitoxigenin, oleandrigenin monodigitoxose, and oleandrigen) compounds with the largest residuals for mAbs 11E6, 5C2, and 40-50, respectively, were removed from the sets (see footnote c in Table 3A) and the target q^2 and r^2 values were achieved (Table 4).

CoMFA Contour Plots. The steric and electrostatic CoMFA StDev*Coeff contour plots, generated with each 3D-QSAR model, identify the regions around the ligands where a change in the field parameters affects the ligand binding activity. Specifically, at each lattice point, the standard deviation of each field value at that point and the corresponding coefficient are multiplied together. If the values are higher than 80% or lower than 20% of all of the calculated products, the point is color-coded and plotted. Green and yellow colors indicate regions where increased steric bulk corresponds to an increase or decrease in the binding affinity, respectively. Red and blue colors indicate regions where an increase in the ligand's negative charge or potential corresponds to an increase or decrease in the binding affinity, respectively.

CoMFA Contour Plot Alignment with X-ray Structure of Fab 40-50–Ouabain Complex. The B and C rings of the representative digoxin molecule in the steric and electrostatic contour plots were aligned with the B and C rings of ouabain in the X-ray structure of the Fab 40-50–ouabain complex (PDB, 1IBG). This matched the CoMFA contour plot regions with the areas occupied by the residues in the Fab 40-50 antigen binding site.

Reagents and Inhibitors. The inhibitors were obtained from the following companies: α-acetyldigoxin, 16-acetylgitoxin, dihydrodigitoxin, and evomonoside were from Indofine; uzarigenin was from Pfalz and Bauer; digitoxigenin bis-digitoxoside, digitoxigenin monodigitoxoside, and digoxigenin bis-digitoxoside were from Roth Karlsrutte; digoxigenin mono-digitoxoside was from Glaxo-Wellcome; acetyldigitoxin, 17α-hydroxyprogesterone 17-acetate 3-(O-carboxymethyl)oxime, acetylstrophanthidin, aldosterone, androsterone, bufalin, chlormadinone acetate, cinobufagin, corticosterone, cortisone, dehydroisoandrosterone, digitoxigenin, digitoxin, digoxigenin, digoxigenin-3,12-diacetate, digoxin, β-estradiol, gitoxigenin, gitoxin, helveticoside, lanatoside C, neriifolin, oleandrin, ouabagenin, ouabain, prednisolone 21-acetate, prednisolone 21-hemisuccinate, progesterone, proscillaridin A, strophanthidin, testosterone, and thevetin B were from Sigma-Aldrich Co. The radioligands, [³H]digoxin and [³H]digitoxin (specific activity 19.0 and 15.9 Ci/mmol, respectively) were from Dupont New England Nuclear, Boston, MA. The affinity-purified goat antihuman IgG Fc specific antibody and rabbit antigoat IgG antibody were from ICN Biomedicals. All other buffers and chemical reagents were purchased from Sigma Chemical Co.

Results and Discussion

Characterization of the Isotype, Binding Avidity, Affinity, and Specificity of Human Sequence Antidigoxin mAb 1B3. After the generation of the six hybridoma cell lines secreting the human sequence antidigoxin mAbs reported previously,[12] we generated and cloned a seventh hybridoma, designated 1B3-18, that secretes an antidigoxin mAb. Using previously reported ELISA methods,[12] we established that mAb 1B3 is a digoxin specific human IgG$_1$ (κ) immunoglobulin with an avidity value of about 1 nM for digoxin.

Next, we determined that ligand binding by mAb 1B3 is distinct from that of the previously characterized human sequence antidigoxin mAbs. First, in a competitive ELISA, 1B3 exhibited a 3-fold higher affinity for digitoxin than for digoxin, the hapten of the immunogen. This higher affinity was confirmed in radioligand binding assays, using [³H]digitoxin and [³H]digoxin, that determined the K_D values to be 0.6 and 3.1 nM, respectively (Table 1). Radioligand competition binding
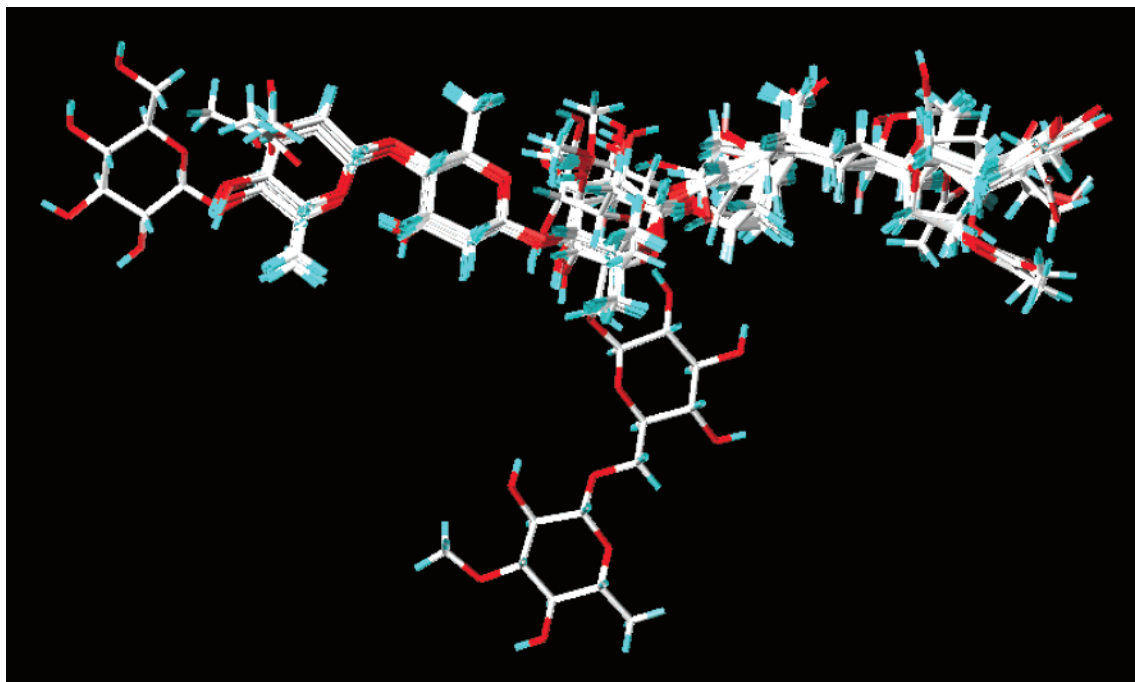
Figure 3. Composite figure of the alignment of cardiotonic and hormonal steroids at the B and C rings.

assays (Table 1) also established that mAb 1B3 has a subnanomolar affinity for digitoxin (K_I = 0.2 nM) as compared to that for digoxin (K_I = ~1 nM). The K_I affinity values were consistently slightly higher than the K_D determinations. For 7F2, 11E6, and 5C2, our previous results showed that removal of the C-12 hydroxyl from digoxin (as in digitoxin) lowered the ligand's affinity 1–5-fold.[12]

Another unique characteristic of 1B3 is the importance of the proximal sugar ring of the ligand for binding. The K_I values of 1B3 for digoxigenin and digitoxigenin were determined against both [³H]digoxin and [³H]digitoxin. These results showed that the relative binding affinity for the aglycones decreased by 3 orders of magnitude for both digoxin and digitoxin (Table 1). This result contrasts dramatically with those for 7F2, 11E6, and 5C2 whose affinities for digoxigenin decreased only 3–13-fold over those for digoxin.[12] Also, 1B3 bound progesterone, a hormonal steroid, with 4 orders of magnitude lower affinity than digoxin; the other three mAbs bound progesterone with 2 orders of magnitude lower affinity. The binding properties of 1B3 demonstrated that despite the potential limitations in their reconstituted "human" immune systems, the transgenic mice can produce antibodies that bind digoxin with different mechanisms. We then proceeded to further analyze these differences.

Analysis of the Competition ELISA Results. The IC$_{50}$ values of the mAbs 1B3, 7F2, 11E6, and 5C2 for a collection of cardiotonic and hormonal steroids (see Figure 1A,B and Table 2A,B for structures) were determined with a competition ELISA (Figure 2 shows selected curves for 1B3 and 7F2). The 1B3 competition binding data are presented for the first time while the data for 7F2, 11E6, and 5C2 are expansions upon those previously reported.[12] Table 3A,B reports all of the compiled results as the IC$_{50}$ ratios.

Simple inspection of the IC$_{50}$ ratios reveals certain trends about the contributions of the sugar, steroid, and lactone moieties to the binding affinity of the human sequence mAbs for the various ligands. Clearly, for 1B3, the proximal sugar is very important for ligand binding. The affinity of 1B3 for digitoxin (IC$_{50}$ ratio of 0.3) is 3 orders of magnitude higher than the affinity for the aglycone digitoxigenin (IC$_{50}$ ratio of 1800). In contrast, the other three human sequence mAbs have only a 1–8-fold higher affinity for digitoxin than the aglycone. It is also interesting that with all four mAbs, removal of the two terminal digitoxose sugars from digoxin has less effect on the affinities than does removal of the same sugars from digitoxin. These results indicate that for 1B3, the proximal sugar is a major contributor to binding ligands while for all four human mAbs, the extent of the contribution of each sugar to the binding affinity also depends on the structure of the steroid moiety.

Furthermore, changes in the conformation and substituents on the four rings of the cardiotonic steroid moiety also affect the ligands' affinities for the human sequence mAbs. For all four human mAbs, when the cardiotonic steroid conformation of the A–B ring cis junction is changed to the hormonal steroid trans conformation (compare digitoxigenin to uzarigenin), the affinity changes only 2–4-fold. Somewhat unexpectedly, 7F2, 11E6, and 5C2 bind uzarigenin better than digitoxigenin, suggesting that the ring orientation of the A–B ring junction does not seem to be a major cause of the antibodies' low affinity for the hormonal steroids. Increasing the hydrophilicity of the cardiotonic steroid base (compare helveticoside and ouabain to digitoxigenin monodigitoxoside), however, decreases the affinity of the four human sequence mAbs from 100–1000-fold or more. More modest changes such as the addition of a hydroxyl at C-12 (compare digoxin to digitoxin) changes the affinity 2–10-fold while addition of a hydroxyl at C-16 (compare gitoxin to digitoxin) lowers the affinity by 10–40-fold. The substitution of a six member lactone ring (bufalin and proscillaridin) for the

Table 3. Compilation of the IC$_{50}$ Ratios for Four mAbs (1B3, 7F2, 11E6, and 5C2) and Rel. K_i for One Murine mAb (40-50) for Various Cardiotonic Steroids and Hormonal Steroids

Section A: Cardiotonic Steroids

| | IC$_{50}$ ratio[a] | | | | rel. K_i[b] |
| | human mAbs | | | | murine mAb |
cardiotonic steroid	1B3	7F2	11E6	5C2	40-50
12-acetyldigoxin					0.5
α-acetyldigoxin	0.9	1	1.5	0.9	
acetyldigitoxin	3.9	25	20	48	
16-acetylgitoxin	49	330	400	290	58
3-epidigoxigenin					12
acetylstrophanthidin	600	17	18	44	10
acovenoside A					0.5
bufalin	6700	550	260	250	
cinobufagin	98000	1700	800	570	
diginatin					33
digitoxigenin	1800	16	14	14	2[c]
digitoxigenin bis-digitoxose	4.9	14	11	14	
digitoxigenin monodigitoxose	36	29	25	47	
digitoxin	0.3	8.0	1.7[c]	10	1
digoxigenin	2700	4.6	6.2	2.9	2
digoxigenin-3,12-diacetate	70	110	96[c]	140[c]	0.7
digoxigenin bis-digitoxose	1.6	1.0	0.9	1.3	
digoxigenin monodigitoxose	5.9	1.0	0.9	1.3	0.6
digoxin	1.0	1.0	1.0	1.0	1
dihydrodigitoxin	340	1800			
dihydrodigoxigenin					300
dihydrodigoxin					280
evomonoside	40	22	29	21	0.6
gitaloxin					35
gitoxigenin	4700	2000	2100	2700	93
gitoxigenin-3-acetate					74
gitoxin	11	81	73	130	16
helveticoside	6200	2100	2500	3000	
lanatoside C	1.6	1.4	1.6	1.1	
neriifolin	69	9.5	17	21	1
oleandrigenin					8600[c]
oleandrigenin monodigitoxose					4[c]
oleandrin	180	3200	3100	ni[d]	200
ouabagenin	52000	13000	6600	ni	9
ouabain	4100	39 000	38000	ni	7
proscillaridin A	670	69	800	400	
strophanthidin	3000	84	66	470	4
strophanthidol					4
strospeside					35
thevetin B	97	8.6	18	7.6	
uzarigenin	4900	4.1	6.7	3.6	

Section B: Hormonal Steroids

| | ratio of IC$_{50}$[e] values | | | |
| | human sequence mAbs | | | |
hormonal steroid	1B3	7F2	11E6	5C2
aldosterone	ni[f]	540	760	550
androsterone	ni	1300	1800	ni
corticosterone	14000	390	970	420
dehydrocortisone	ni	ni	ni	3400
hydrocortisone	ni	1100	3700	650
prednisolone 21-acetate	ni	12 000		
prednisolone 21-hemisuccinate	160000	3400		
progesterone	36000	69	100	55
testosterone	ni	100	110	120
17α-hydroxyprogesterone 17-acetate 3-(O-carboxymethyl)oxime	ni	ni		
β-estradiol	ni	ni	ni	ni
chlormadinone acetate	ni	ni		
cholesterol	ni	ni	ni	ni
cortisone	ni	ni	ni	ni
dehydroisoandrosterone	ni			

[a] IC$_{50}$ inhibitor/IC$_{50}$ digoxin. Reported values are the average of 3−7 independent determinations. The average fractional standard error was 0.3. [b] Murine Fab 40-50 data was generated in Margolies' lab.[17] [c] Data points were removed to generate the final model. [d] ni for no inhibition observed with up to 1 mM inhibitor. [e] IC$_{50}$ steroid/IC$_{50}$ digoxin. [f] ni for no inhibition observed up to 1 mM inhibitor.

five member ring or reduction of the double bond in the five-membered lactone (dihydrodigitoxin) also significantly decreases the binding affinity and demonstrates the importance of the cardenolide five member lactone. Finally, the hormonal steroid, progesterone, has a 4−20-fold lower affinity than digitoxigenin for all four human

Table 4. Statistical Analysis and Field Contributions for 3D-QSAR Models (II) of Four Human Sequences and One Murine mAb[a]

mAb	no. of principal components	q^2	r^2	F	n	% steric field contribution	% electrostatic field contribution
1B3	5	0.834	0.974	196	32	43	57
7F2	5	0.532	0.920	72	37	38	62
11E6	5	0.594	0.924	63	32	39	61
5C2	4	0.570	0.908	62	30	37	63
40-50	6	0.534	0.986	210	25	41	59

[a] n = number of compounds in data sets.

mAbs. In fact, most of the hormonal steroids (which lack the lactone ring) bind very weakly or not at all.

We should also point out that there may be minor differences in the orientation of some ligands within the mAbs binding sites. For example, the addition of a digitoxose sugar to strophanthidin (generating helveticoside) significantly decreases the relative binding affinity of the ligand with mAb 7F2 (84−2100; a 27-fold decrease). In contrast, the addition of a single digitoxose to digitoxigenin or digoxigenin results in a 2-fold lower or 5-fold higher affinity, respectively. It could be that the oxygen atoms at the C-5, C-12, and C-19 may change the orientation of the ligand in the binding site such that the addition of the digitoxose to different ligands has a different effect on the mAbs 7F2 affinity.

These observations about the contributions of the sugars, the steroid ring structure, and the lactone ring to antibody−ligand complex formation were analyzed further by producing 3D-QSAR models (see Figure 3 for compound alignment) and contour plots.

Preliminary 3D-QSAR Models and Test Sets. To produce statistically satisfactory models, a few compounds (see Table 3A,B and Materials and Methods) were excluded from the 3D-QSAR analysis. In particular, for mAbs 11E6 and 5C2 digoxigenin-3,12-diacetate and for 40-50, the oleandrins proved difficult to model. Once these compounds were removed, we used the training set data to produce model I for each mAb and these models were able to generate good predictions for half or more of the test set compounds (see Figure 4A,B).

CoMFA Contour Plots for Human Sequence mAbs. The CoMFA contour plots were developed from model II, the final 3D-QSAR models. Figure 4A,B shows for 1B3 and 7F2 the correlation between the observed relative affinities and the corresponding CoMFA predicted values (insets show q^2 plots). The plots highlight the wide range and even distribution of the activities. The self-consistency and predictive capability of the developed models are examined using several statistical parameters, as summarized in Table 4. A review of the parameters shows that 1B3, 7F2, and 11E6 required five PCs to explain the variance in the IC$_{50}$ ratios while the models for 5C2 and 40-50 required four and six PCs, respectively. All of the models gave q^2 values greater than 0.5 and r^2 values greater than 0.9, demonstrating that they all reached or exceeded generally accepted criteria for good predictability and consistency. In addition, the steric and electrostatic fields made similar contributions, ∼40 and ∼60%, respectively, to all of the antidigoxin mAb models.

Contour Plots for mAb 1B3. The CoMFA steric contour plot for mAb 1B3 is shown in Figure 5A, with digoxin inserted as the reference molecule. A green, irregular donutlike region surrounds the proximal digi-
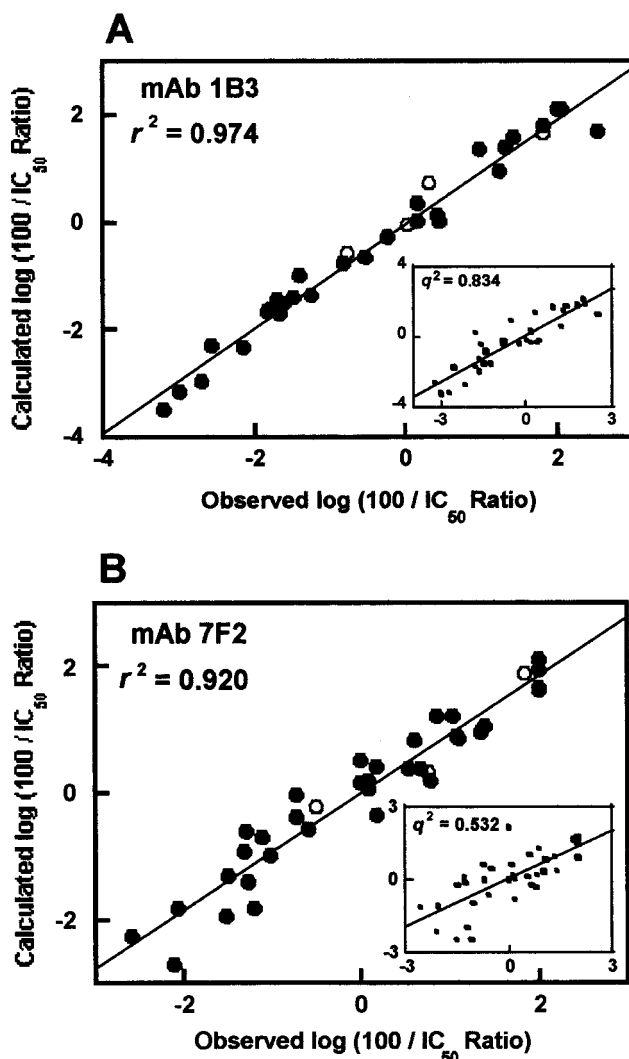
Figure 4. Comparison of the CoMFA predicted log(100/IC$_{50}$ ratio) values with the experimentally determined log(100/IC$_{50}$ ratio) values for 1B3 (A) and 7F2 (B). The r^2 for 1B3 data was 0.97; the q^2 was 0.83 with the correlation plot shown in inset. The r^2 for 7F2 was 0.92; the q^2 was 0.53 as shown in inset. The plotted values for the test set compounds omitted in model I are given as open circles in panels A and B.

toxose sugar and highlights the space where increased steric bulk on the ligand is favorable for binding. This field is consistent with the observed importance for at least one sugar to be present at C-3. For example, the ligand's affinity is increased by 2−3 orders of magnitude when the digitoxose groups are added to digoxigenin and gitoxigenin. In addition, the monosugar compounds digitoxigenin-monodigitoxose, evomonoside (monorhamnose), and neriifolin (monothevetose), also showed improvement in their affinities (IC$_{50}$ ratios are 36, 40, and 69, respectively), as compared to digitoxigenin (IC$_{50}$ ratio is 1800). Therefore, this green region suggests that
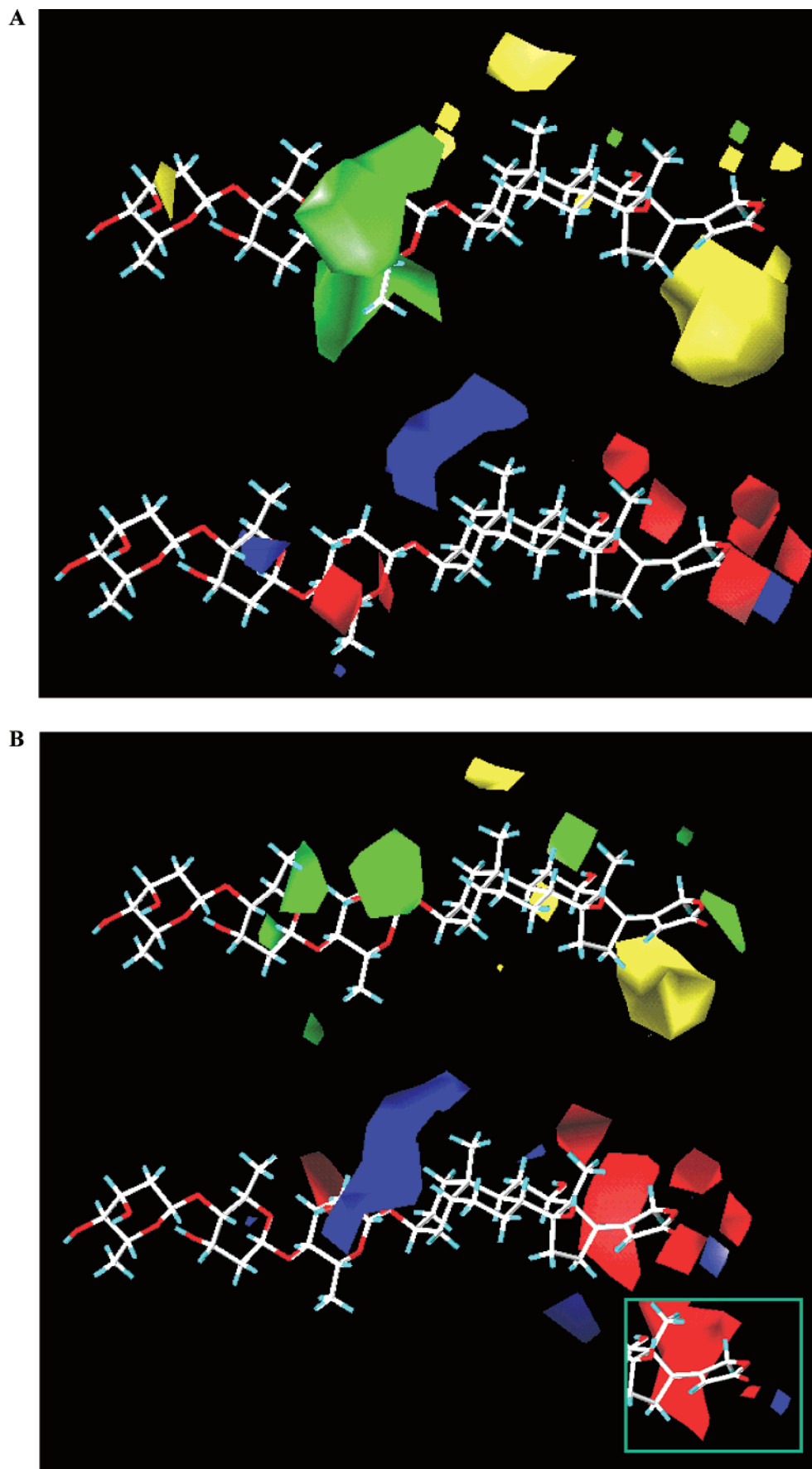
Figure 5. CoMFA contour plots of the steric and electrostatic field contributions of ligand binding to mAbs (A) 1B3 and (B) 7F2. The addition or subtraction of steric bulk in regions of green or yellow color, respectively, will increase the binding affinity. The addition or subtraction of negative charge or potential in regions of red or blue color, respectively, will also increase the binding affinity. The boxed insert (in B) shows the region around the lactone ring of mAb 11E6. Digoxin is inserted as a reference ligand.

there is an area of the mAb 1B3's binding site that interacts with the proximal sugar but does not discriminate its exact structure.

The yellow regions near the steroid backbone and lactone ring identify regions where adding bulk to the ligand decreases affinity. This is supported by the data for helveticoside, ouabain, and oleandrin (as compared to digitoxigenin monodigitoxoside) as well as bufalin and cinobufagin (as compared to digitoxigenin). Repositioning the five member lactone ring by saturating the double bond (dihydrodigitoxin vs digitoxin) also decreases the binding affinity for 1B3. Specific mAb residues probably make close contact with the high affinity ligands near these yellow areas; therefore, changes in the ligand's shape decrease the effectiveness of the contact.

Electrostatic interactions make the major contribution (57%) to the 1B3 3D-QSAR model, and the blue and red contour plot regions visualize where these interactions occur. The largest blue region covering the first glycosidic bond and the steroid A ring identifies a space where an increase in the electropositivity of the ligand increases the binding affinity. For example, digitoxigenin has an IC_{50} ratio of 1800. If a sugar is added [monodigitoxose, evomonoside (monorhamnose), or neriifolin (monothevetose)], the affinity increases 30–50-fold. Perhaps a hydroxyl group on the sugar is participating in a hydrogen bonding with a residue in the mAb. However, blue can also designate regions where an increase in electronegativity decreases affinity. For example, helveticoside, with oxygen atoms at C-5 and C-19, and ouabain, with oxygen atoms at C-1, C-5, C-11, and C-19 (that are absent in digitoxigenin), both have a much lower affinity than digitoxigenin monodigitoxoside. In addition, the presence of oxygen at the steroid C-5 and C-19 positions changes the effects of the proximal sugar. Consider the following drug pairs: digitoxigenin and digitoxigenin monodigitoxoside vs strophanthidin and strophanthidin monodigitoxoside (helveticoside). In the first case, the addition of the sugar improves the affinity by 50-fold. In the second case, the addition decreases the affinity 2-fold. The addition of the digitoxose sugar had a negative effect on the affinity when oxygen atoms at C-5 and C-19 were present. Furthermore, it is unclear why the addition of an acetyl group to strophanthidin increases the affinity 5-fold although the addition of digitoxose decreases the affinity. Modest alterations in the orientation of the ligand may determine which residue(s), of several possible residues within the mAb binding site, is (are) able to bind to the sugar. The two red-blue tinged regions located on the α, or topside surface of the steroid moiety (rings C and D) as commonly viewed, are more difficult to explain since the hydroxyl group at C-12 modestly increases (digoxigenin monodigitoxose) or decreases (digoxin) the affinity, dependent upon which sugars are present. Finally, we also point out the cluster of fields, including a red and blue pair of electrostatic regions, about the lactone ring that will be discussed below.

Contour Plots for Human mAbs 7F2, 11E6, and 5C2. Despite the fact that the radioligand binding data[12] indicate that the digoxin binding affinities of mAbs 7F2 and 11E6 are higher than 5C2, the patterns of their IC_{50}

ratios are quite similar for these three mAbs and distinct from 1B3. The 3D-QSAR analyses further indicate this distinction in that they have similar lower q^2 values for their models than 1B3 and they have a different distribution pattern to their PC values. Also, the relative steric−electrostatic field contributions to the 3D-QSAR models and their contour plots are quite similar. Removing the three sugars from digoxin and digitoxin has a relatively small effect on their IC_{50} ratios, especially as compared to the values for mAb 1B3. Clearly, for 7F2, 11E6, and 5C2, their contour plots show separate, localized green regions about the two proximal sugars. One might conclude that the binding sites of these three mAbs have less interaction with this region of digoxin than does the mAb 1B3. In contrast, all four mAbs show a similar, ∼10-fold or more decrease in the binding affinity for gitoxin (C-16 hydroxyl) relative to digitoxin and a further 2−5-fold decrease in the affinity for 16-acetylgitoxin relative to gitoxin. Also, their steric contour plots about the latter portion of the ligand are similar, especially the large yellow region near the steroid C-16 and lactone ring, which indicate a close fit between mAb and ligand.

We propose that specific differences in the contour plots should reflect differences in the residues of the mAbs' binding site. Like 1B3, models for 7F2 and 5C2 show a cluster of red regions and a blue and red-paired region near the lactone ring. mAb 11E6, despite IC_{50} ratios almost identical to 7F2, has a simpler pattern (insert in Figure 5B). In fact, because the IC_{50} ratios for 7F2 and 11E6 (except for proscillaridin A) were so similar and they are secreted by hybridomas obtained from the same mouse, we suspected that they might be the same antibody, secreted by sibling clones. However, while both bufalin and proscillaridin A have a six member lactone ring and the bufalin IC_{50} ratios for 7F2 and 11E6 were fairly similar (550 and 260, respectively), addition of the rhamnose sugar and a double bond in the steroid A ring that changed the orientation of the bound ligand caused the affinity of 7F2 for proscillaridin A to increase (IC_{50} ratio is 69) but the affinity of 11E6 decreased (IC_{50} ratio is 800). The grouping of blue and red regions located near the lactone ring in 7F2 suggests electrostatic interactions that are not available for 11E6.

Although 7F2 and 1B3 have similar affinities for digoxin, 7F2 is more sensitive to structural changes on the steroid moiety than is 1B3. The aglycones, digitoxigenin, strophanthidin, bufalin, and gitoxigenin all lack sugar groups and differ from digoxigenin at the steroid C-12; C-5, C-12, and C-19; C-12 and C-17; and C-12 and C-16 sites, respectively. For 7F2, the digoxigenin-based IC_{50} ratios for the above compounds were 3.5, 18, 120, and 430, respectively. For 1B3, although the affinities were low, the IC_{50} ratios were all similar. In addition, because (unlike 1B3) the affinity of mAb 7F2 is less dependent on the presence or type of sugar at C-3, it is able to recognize a number of hormonal steroids although their affinities are 2 orders of magnitude lower than those for digoxin or digitoxin.

mAb 5C2, which had the poorest affinity for digoxin, also initially generated the model with the lowest predictive ability and required the omission of one compound. In an attempt to improve the predictive ability of the 5C2 model, we increased the fineness of
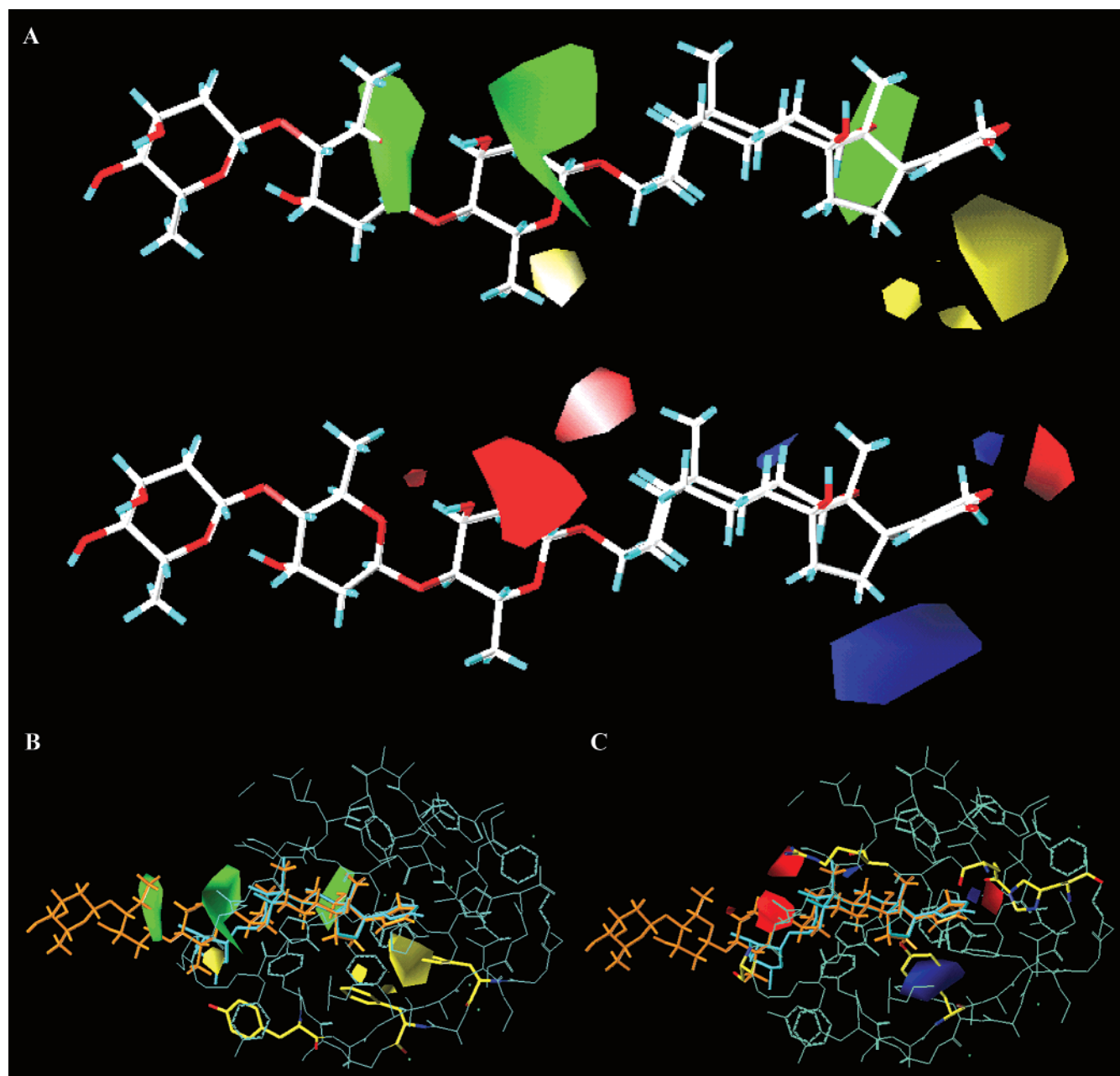
Figure 6. CoMFA contour plots of the steric and electrostatic field contributions of ligand binding to mAb 40-50 with digoxin inserted as the reference ligand. (A) Steric and electrostatic fields are presented separately. (B) The steric contour plot is matched with the X-ray crystal structure of the binding site of 40-50. The addition or subtraction of steric bulk in regions of green or yellow color, respectively, will increase the binding affinity. (C) The electrostatic contour plot is matched with the binding site of 40-50. The addition or subtraction of negative charge in regions of red or blue color, respectively, will increase the binding affinity. Digoxin (orange) is inserted as the reference ligand in these contour plots and is aligned with ouabain (teal), the ligand present in the X-ray crystal structure.

the grid spacing to 1 Å. However, there was no improvement in the calculated q^2 value. This lack of q^2 improvement with a smaller grid spacing is consistent with the results from other CoMFA studies.[23]

Contour Plot for Murine mAb 40-50. Next, we generated a 3D-QSAR model and contour plot for the mouse antidigoxin mAb 40-50 using previously obtained data of its binding to 28 cardiotonic glycosides.[17] We then compared its 3D-QSAR model with those of the human mAbs and matched the generated contour plot with the known structure of ouabain in the 40-50 binding site.[17] The individual contributions to 40-50's 3D-QSAR model from the steric and electrostatic fields were 41 and 59%, respectively, which is similar to the

results for three of the human sequence mAbs. The main decrease in its binding affinity occurs with the modifications at the steroid C-16 position (gitoxin, oleandrin, and their analogues) and saturation of the lactone ring (dihydrodigoxin and dihydrodigoxigenin). The contour plot for the steric interactions shows a yellow region near the D ring at C-16, which is consistent with the decrease in affinity with an increase in steric bulk at this position. The large yellow region below the lactone ring suggests that a change in orientation of the lactone ring upon reduction of the double bond also decreases the binding affinity.

Next, we aligned the digoxin molecule and the CoMFA steric contour plot with ouabain in the Fab 40-50–

Table 5. Comparison of Contact Residues for Antidigoxin mAb 40-50[17] and Antiprogesterone Fab′ DB3[38] [a]

Fab	Residues		
	CDR I	CDR II	CDR III
	LIGHT CHAIN		
	27d 32		9192 94 96
40-50	RASKSVS**T**_SGYS**H**IH … LASILES …		Q**H**S**R**E**Y**PL**T**
	27d		9192 94 96
DB3	RSSQSLI**H**SNGNTYLH … KVSNRFY …		S**Q**S**S**HVP**PT**
	HEAVY CHAIN		
	35 50 52		95 97 100 100a 100c 100e
40-50	TYGV**H** … **L**I**W**AGGNTDYNSALMS …		**F**R**F**AS**YYD**Y**A**VDY
	35 50		95 96 97 100 100b
DB3	NYGV**N** … **W**INIYTGEPTYVDDFKG …		**GD**Y**V**N**W**Y**F**---DV

[a] Contact residues of 40-50 and DB3 for ouabain and progesterone, respectively, identified by sequence number.

ouabain complex structure. Consistent with their crystallographic identifications as contact residues, the aligned plots show that Phe-H95, Phe-H97, and Tyr-H100A are likely to contribute to the generation of the close fit between antibody and ligand. These side chains would present large hydrophobic surfaces to the ligand and restrict any increase in the size of the ligand in this area (Figure 6B).

The contour plot for the electrostatic interactions also shows a blue region near the steroid's D ring at C-16, which is consistent with the observed decrease in affinity that occurs after substitutions of hydroxyl or acetate groups. The hydroxyl of the Tyr-H100c could be responsible for the blue area. Interestingly, the blue-red paired region near the keto group of the lactone ring is similar to that observed for the human mAbs 1B3, 7F2, and 5C2. The HisH-35 and GlnL-89 of 40-50 may provide the required electrostatic interactions (Figure 6C), respectively.

The contour plots also show green, yellow, and red regions near the C-3 proximal glycosidic bond and sugar. The rel. K_i data suggest that the gitoxin-related compounds are more sensitive to the presence (or type) of sugar moieties at C-3 than are digoxin-related compounds. For example, there is only a 2-fold difference in the rel. K_i for digoxin, digoxigenin, digitoxin, and digitoxigenin. Nevertheless, there is a 6-fold increase in affinity for gitoxin over gitoxigenin and a 50-fold increase in affinity for oleandrigenin monodigitoxose over oleandrin (oleandrose sugar). Because the sugars can rotate, the residues that are responsible for generating the contour plot may not be precisely adjacent to the corresponding color-coded fields. The red regions could represent areas where Arg-L92 or Ser-L28 interact with the ligand oxygen atoms or where tyrosines donate their protons for hydrogen bonding (Figure 6C).

Extending our analysis of the contact residues of the antidigoxin mAb 40-50 with those determined by Wilson and colleagues[38] for the antiprogesterone mAb DB3 suggests that there may be general requirements for antibody binding sites for steroids. Table 5 shows that the CDR regions of both Fabs 40-50 and DB3 have a high frequency of aromatic residues and that the contact residues for ouabain and progesterone are located in similar sequence positions. Tyrosine and tryptophan together represent eight of the 27 contact residues identified. Because these two residues are capable of

forming both hydrophobic and electrostatic interactions, they have been implicated as being responsible for broadening antibody cross-reactivity.[24,33] It seems likely that mAbs 7F2, 11E6, and 5C2, which bind both digoxin and progesterone, also have their ligand contact residues located in similar positions.

Conclusions

The HC2/KCo5 transgenic mice, with their reconstructed, humanized immune system, are able to generate human antidigoxin mAbs with varying digoxin-binding mechanisms and a complexity that can match that of normal mouse mAbs. For example, the proximal sugar has a major role in determining the binding affinity of 1B3 when compared to the previously characterized human mAbs. Furthermore, once the sugars are removed, substitutions on the steroid and lactone moieties have modest effects on binding affinity for 1B3. For the other three human mAbs, the steroid−lactone moieties have a larger role in complex formation. 3D-QSAR models can be developed for these antibody−ligand interactions, and the CoMFA contour plots can visualize the steric and electrostatic fields that are important for binding.

Because these fields can indicate which amino acid residues in the binding site for the ligand are important for complex formation, we propose that 3D-QSAR models will be useful tools in the development of therapeutic antibodies by yielding information that enables us to improve antibody affinity or specificity. Redesigned therapeutic antibodies could include either a broadened or more limited specificity, i.e., an antibody that has a high affinity for digoxin, digitoxin, oleandrin, and bufalin or modified antibodies that are specific for each of these compounds. These mAbs could permit improved diagnosis and treatment in cases of cardenolide overdoses or bufalin poisonings. Once we complete the sequencing of these human mAbs, we should be able to generate molecular models of their digoxin binding sites. Then, we can compare the CoMFA contour plot information with the corresponding binding site models. This information will help us to better understand the mechanisms of the mAb−ligand interactions and to design improved therapeutic and diagnostic agents.

References

(1) National Health and Nutrition Examination Survey III (NHANES III) 1988−94; American Center for Disease Control (CDC)/NCHS data 1979−96.
(2) Reddy, S.; Benatar, D.; Gheorghiade, M. Update on Digoxin and Other Oral Positive Inotropic Agents for Chronic Heart Failure. *Curr. Opin. Cardiol.* **1997**, *12*, 233−241.
(3) IMS Health at http://www.rxlist.com/top200.htm, February 28, 2001.
(4) Soler-Soler, J.; Permanyer-Miralda, G. Should We Still Prescribe Digoxin in Mild-to-Moderate Heart Failure? *Eur. Heart J.* **1998**, *19* (Suppl. P), 26−31.
(5) Erdmann, E. The Effect of Positive Inotropes on the Failing Human Myocardium. *Cardiology* **1997**, *88* (Suppl. 2), 7−11.

(6) Smith, T. W.; Antman, E. M.; Friedman, P. L.; Blatt, E. M.; Marsh, J. G. Digitalis Glycosides: Mechanisms and Manifestations of Toxicity. *Prog. Cardiovasc. Dis.* **1984**, *26*, 413−458.

(7) Smith, T. W.; Butler, V. P., Jr.; Haber, E.; Fozzard, H.; Marcus, F. I.; Bremner, W. F.; Schulman, I. C.; Phillips, A. Treatment of Life-Threatening Digitalis Intoxication with Digoxin-Specific Fab Antibody Fragments. *N. Engl. J. Med.* **1982**, *307*, 1357−1362.

(8) Butler, V. P., Jr.; Chen, J. P. Digoxin-Specific Antibodies. *Proc. Natl. Acad. Sci. U.S.A.* **1967**, *57*, 71−78.

(9) Bismuth, C.; Borron, S. W.; Baud, F. J.; Taboulet, P.; Scherrmann, J.-M. Immunotoxicotherapy: Successes, Disappointments and Hopes. *Hum. Exp. Toxicol.* **1997**, *16*, 602−608.

(10) Borron, W. W.; Bismuth, C.; Muszynski, J. Advances in the Management of Digoxin Toxicity in the Older Patient. *Drugs Aging* **1997**, *10*, 18−33.

(11) Scherrmann, J.-M. Antibody Treatment of Toxin Poisoning−Recent Advances. *Clin. Toxicol.* **1994**, *32*, 363−375.

(12) Ball, W. J., Jr.; Kasturi, R.; Dey, P.; Tabet, M.; O'Donnell, S.; Hudson, D.; Fishwild, D. Isolation and Characterization of Human Monoclonal Antibodies to Digoxin. *J. Immunol.* **1999**, *163*, 2291−2298.

(13) Padlan, E. A. Anatomy of the Antibody Molecule. *Mol. Immunol.* **1994**, *31*, 169−217.

(14) Schildbach, J. F.; Panka, D. J.; Parks, D. R.; Jager, G. C.; Novotny, J.; Herzenberg, L. A.; Mudgett-Hunter, M.; Bruccoleri, R. E., Haber, E.; Margolies, M. N. Altered Hapten Recognition by Two Anti-Digoxin Hybridoma Variants Due to Variable Region Point Mutations. *J. Biol. Chem.* **1991**, *266*, 4640−4647.

(15) Mudgett-Hunter, M.; Anderson, W.; Haber, E.; Margolies, M. N. Binding and Structural Diversity Among High-Affinity Monoclonal Anti-Digoxin Antibodies. *Mol. Immunol.* **1985**, *22*, 477−488.

(16) Schildbach, J. F.; Near, R. I.; Bruccoleri, R. E.; Haber, E.; Jeffrey, P. D.; Ng, S.-C.; Novotny, J.; Sheriff, S.; Margolies, M. N. Heavy Chain Position 50 is a Determinant of Affinity and Specificity for the Anti-Digoxin Antibody 26−10. *J. Biol. Chem.* **1993**, *268*, 21739−21747.

(17) Jeffrey, P. D.; Schildbach, J. F.; Chang, C. Y. Y.; Kussie, P. H.; Margolies, M. N.; Sheriff, S. Structure and Specificity of the Anti-Digoxin Antibody 40−50. *J. Mol. Biol.* **1995**, *248*, 344−360.

(18) Jeffrey, P. D.; Strong, R. K.; Sieker, L. C.; Chang, C. Y. Y.; Campbell, R. L.; Petsko, G. A.; Haber, E.; Margolies, M. N.; Sheriff, S. 26-10 Fab-Digoxin complex: Affinity and Specificity Due to Surface Complementarity. *Proc. Natl. Acad. Sci. U.S.A.* **1993**, *90*, 10310−10314.

(19) Cramer, R. D., III; Patterson, D. E.; Bunce, J. D. Comparative Molecular Field Analysis (CoMFA). 1. Effect of Shape on Binding of Steroids to Carrier Proteins. *J. Am. Chem. Soc.* **1988**, *110*, 5959−5967.

(20) Green, S. M.; Marshall, G. R. 3D-QSAR: a Current Perspective. *TiPS* **1995**, *16*, 285−291.

(21) Tong, W.; Perkins, R.; Strelitz, R.; Collantes, E. R.; Keenan, S.; Welsh, W. J.; Branham, W. S.; Sheehan, D. M. Quantitative Structure−Activity Relationships (QSARs) for Estrogen Binding to the Estrogen Receptor: Predictions Across Species. *Environ. Health Perspect.* **1997**, *105*, 1116−1124.

(22) Tong, W.; Lowis, D. R.; Perkins, R.; Chen, Y.; Welsh, W. J.; Goddette, D. W.; Heritage, T. W.; Sheehan, D. M. Evaluation of Quantitative Structure−Activity Relationship Methods for Large-Scale Prediction of Chemicals Binding to the Estrogen Receptor. *J. Chem. Inf. Comput. Sci.* **1998**, *38*, 669−677.

(23) Tong, W.; Perkins, R.; Xing, L.; Welsh, W, J.; Sheehan, D. M. QSAR Models for Binding of Estrogenic Compounds to Estrogen Receptor α and β Subtypes. *Endocrinology* **1997**, *138*, 4022−4025.

(24) Gamper, A. M.; Winger, R. H.; Liedl, K. R.; Sotriffer, C. A.; Varga, J. M.; Kroemer, R. T.; Rode, B. M. Comparative Molecular Field Analysis of Haptens Docked to the Multispecific Antibody IgE-(Lb4). *J. Med. Chem.* **1996**, *39*, 3882−3888.

(25) Imberty, A.; Mollicone, R.; Mikros, E.; Carrupt, P.-A.; Pérez, S.; Oriol, R. How do Antibodies and Lectins Recognize Histo-Blood Group Antigens? A 3D-QSAR Study by Comparative Molecular Field Analysis (CoMFA). *Bioorg. Med. Chem.* **1996**, *4*, 1979−1988.

(26) Shim, J.-Y.; Collantes, E. R.; Welsh, W. J.; Subramaniam, B.; Howlett, A. C.; Eissenstat, M. A.; Ward, S. J. Three-Dimensional Quantitative Structure−Activity Relationship Study of the Cannabimimetic (Aminoalkyl)indoles Using Comparative Molecular Field Analysis. *J. Med. Chem.* **1998**, *41*, 4521−4532.

(27) Collantes, E. R.; Xing, L.; Miller, P. C.; Welsh, W. J.; Profeta, S., Jr. Comparative Molecular Field Analysis as a Tool to Evaluate Mode of Action of Chemical Hybridization Agents. *J. Agric. Food Chem.* **1999**, *47*, 5245−5251.

(28) Collantes, E. R.; Tong, W.; Welsh, W. J. Use of Moment of Inertia in Comparative Molecular Field Analysis to Model Chromatographic Retention of Nonpolar Solutes. *Anal. Chem.* **1996**, *68*, 2038−2043.

(29) Go, K.; Kartha, G.; Chen, J. P. Structure of Digoxin. *Acta Crystallogr.* **1980**, *B36*, 1811−1819.

(30) Arevalo, J. H.; Hassig, C. A.; Stura, E. A.; Sims, M. J.; Taussig, M. J.; Wilson, I. A. Structural Analysis of Antibody Specificity−Detailed Comparison of Five Fab'-Steroid Complexes. *J. Mol. Biol.* **1994**, *241*, 663−690.

(31) Fersht, A. R. Basis of Biological Specificity. *TIBS* **1984**, *9*, 145−147.

(32) Arevalo, J. H.; Taussig, M. J.; Wilson, I. A. Molecular Basis of Crossreactivity and the Limits of Antibody−Antigen Complementarity. *Nature* **1993**, *365*, 859−863.

(33) Mian, I. S.; Bradwell, A. R.; Olson, A. J. Structure, Function and Properties of Antibody Binding Sites. *J. Mol. Biol.* **1991**, *217*, 133−151.

(34) Taylor, L. D.; Carmack, C. E.; Huszar, D.; Higgins, K. M.; Mashayekh, R.; Sequar, G.; Schramm, S. R.; Kuo, C.-C.; O'Donnell, S. L.; Kay, R. M.; Woodhouse, C. S.; Lonberg, N. Human Immunoglobulin Transgenes Undergo Rearrangement, Somatic Mutation and Class Switching in Mice that Lack Endogenous IgM. *Int. Immunol.* **1994**, *6*, 579−591.

(35) Lonberg, N.; Taylor, L. D.; Harding, F. A.; Trounstine, M.; Higgins, K. M.; Schramm, S. R.; Kuo, C.-C.; Mashayekh, R.; Wymore, K.; McCabe, J. G.; Munoz-O'Regan, D.; O'Donnell, S. L.; Lapachet, S. G.; Bengoechea, T.; Fishwild, D. M.; Carmack, C. E.; Kay, R. M.; Huszar, D. Antigen-specific human antibodies from mice comprising four distinct genetic modifications. *Nature* **1994**, *368*, 856−859.

(36) Fishwild, D. M.; O'Donnell, S.; Bengoechea, T.; Hudson, D. J.; Harding, F. High-avidity Human IgG κ Monoclonal Antibodies from a Novel Strain of Minilocus Transgenic Mice. *Nat. Biotechnol.* **1996**, *14*, 845−851.

(37) Cheng, Y.-C.; Prusoff, W. H. Relationship Between the Inhibition Constant (K_I) and the Concentration of Inhibitor which Causes 50 Percent Inhibition (I_{50}) of an Enzymatic Reaction. *Biochem. Pharmacol.* **1973**, *22*, 3099−3108.

(38) Arevalo, J. H.; Stura, E. A.; Taussig, M. J.; Wilson, I. A. Three-Dimensional Structure of an Anti-Steroid Fab' and Progesterone-Fab' Complex. *J. Mol. Biol.* **1993**, *231*, 103−118.

(39) Gasteiger, J.; Marsili, M. Iterative Partial Equalization of Orbital Electronegativity−A Rapid Access to Atomic Charges. *Tetrahedron* **1980**, *36*, 3219−3228.